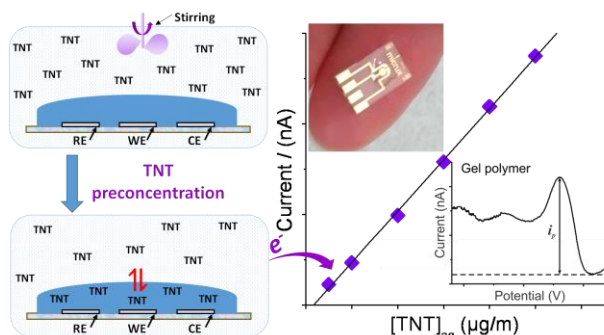


Detection of 2,4,6-trinitrotoluene using a miniaturized, disposable electrochemical sensor with an ionic liquid gel-polymer electrolyte film

Holly A. Yu, Junqiao Lee, Simon W. Lewis, Debbie S. Silvester*

Nanochemistry Research Institute, Department of Chemistry, Curtin University, GPO Box U1987, Perth, Western Australia 6845, Australia

ABSTRACT: A new electrochemical method to detect and quantify the explosive compound 2,4,6-trinitrotoluene (TNT) in aqueous solutions is demonstrated. A disposable thin-film electrode modified with a droplet of a gel-polymer electrolyte (GPE) was immersed directly into samples of TNT at concentrations of 1–10 $\mu\text{g/mL}$. The GPE contained the hydrophobic room temperature ionic liquid (RTIL) trihexyltetradecylphosphonium bis(trifluoromethylsulfonyl)imide ($[\text{P}_{14,6,6,6}][\text{NTf}_2]$) and the polymer poly(hexyl methacrylate) (PHMA). The RTIL acted to pre-concentrate TNT into the GPE, and provided ionic conductivity. The polymer provided both (i) sufficient viscosity to ensure mechanical stability of the GPE, and (ii) strong hydrophobicity to minimise leaching of the RTIL. Square wave voltammetry (SWV) was performed on the first reduction peak of TNT-preconcentrated samples (15 minutes soaking with mechanical stirring), with linear plots of peak current vs. cumulative concentration of TNT, giving an averaged limit of detection of 0.37 $\mu\text{g/mL}$ (aqueous phase concentration). Additionally, the voltammetry of the first reduction peak of TNT in $[\text{P}_{14,6,6,6}][\text{NTf}_2]$ was unaffected by the presence of oxygen – in contrast to that observed in an imidazolium-based RTIL – providing excellent selectivity over oxygen in real environments. The sensor device was able to quickly and easily quantify TNT concentrations at typical groundwater contamination levels. The low-cost and portability of the sensor device, along with the minimal amounts of GPE materials required, make this a viable platform for the onsite monitoring of explosives, which is currently a significant operational challenge.



Introduction

Explosive compounds – often called energetic materials – are widely used in demolition, mining, and for military purposes.¹ In the wrong hands, they can also be used as materials in terrorist attacks. Explosives such as 2,4,6-trinitrotoluene (TNT) are known to penetrate from soil into groundwater as a result of military activities, demolitions, or improper management and disposal practices.¹ TNT and its by-products can contaminate environments to levels that threaten the health of ecosystems, livestock, wildlife and humans (e.g. TNT is carcinogenic).¹ As a result, there has been much interest in developing methods such as mass spectrometry, gas chromatography, and ion mobility spectroscopy to detect TNT for safety and environmental applications.² However, these techniques require bulky and expensive instrumentation, and are often not suitable for onsite analysis. Electrochemical sensors offer a viable alternative

for the rapid onsite screening of redox-active explosive compounds, due to their low-cost, high sensitivity and selectivity, low-power requirements, durability, and instrument portability.^{3,4} They typically require solvents to connect the electrodes, and an electrolyte to carry the charge.

Room temperature ionic liquids (RTILs) are salts made entirely of ions (typically a bulky organic cation and inorganic anion) and have been investigated as a replacement solvent/electrolyte in electrochemical reactions and electrochemical sensors. Since 2009, the electrochemical behaviour and detection of explosives such as TNT in RTILs has been the subject of various studies.⁵⁻⁷ Using cyclic voltammetry, three distinct reduction peaks for TNT have been observed in eight different RTILs.⁸ A one-electron reduction mechanism, followed by dimerization at high concentrations, was proposed for the first reduction peak, resulting in the formation of azo or azoxy compounds.⁸ This is in contrast to that ob-

served in aqueous solutions, where three successive six-electron reduction peaks are observed (each nitro group is reduced to the amine).⁹

From an analytical perspective, the detection of TNT in RTILs has been studied by both vapour phase sampling and direct dissolution. For example, explosive vapours were first detected in RTILs through a hybrid electrochemical-colorimetric sensing platform.¹⁰ The authors suggested that the RTIL acted to preconcentrate the explosives, and that the presence of the RTIL was necessary to produce coloured reduction products that were detected.¹⁰ The same group employed a hybrid nanosensor consisting of a conducting polymer nanojunction with a thin layer of RTIL, to detect TNT vapours down to the parts-per-trillion level.¹¹ Xiao et al.¹² reported the behaviour of both dissolved and vapor phase TNT in four RTILs using square wave voltammetry (SWV). A detection limit of 190 nM was reported for TNT in the liquid phase, and the preconcentration ability of the RTILs was also highlighted. A miniaturized, solid-state 'forensic finger' was used to detect the explosive 2,4-dinitrotoluene (DNT) from gunshot residue.¹³ The sensor was fabricated by screen-printing the electrode onto a flexible substrate, followed by printing of an ionogel (an ionic liquid with a water-soluble diacrylate polymer).

Concerning detection in aqueous solutions, TNT was extracted from aqueous samples into an RTIL by generating an RTIL *in situ* in the sample, using a metathesis reaction.¹⁴ A linear analytical response was observed, with limit of detection of 7 µg/L, however, the sample preparation steps were quite complex for onsite detection. In other work, Guo et al. demonstrated the detection of TNT down to 0.5 ppm using an ionic liquid-graphene paste composite electrode.¹⁵ Another group later employed a glassy carbon electrode modified with ionic liquid-graphene hybrid nanosheets as an enhanced material to rapidly detect TNT.¹⁶ A detection limit of 4 ppm was reported using adsorptive stripping voltammetry, and the setup was applied to real samples such as ground water, tap water and lake water. Vu et al.¹⁷ used differential pulse adsorptive stripping voltammetry at a carbon paste electrode with graphite powder, paraffin oil and an ionic liquid for the detection of TNT. A linear range from 1.5 to 30 ppm was demonstrated, with a detection limit of 88.6 parts per billion, and the sensor showed good stability and reproducibility. Although these studies¹⁵⁻¹⁷ have shown that TNT can be detected in aqueous solutions using RTILs, they employ a relatively large working electrode, and require the use of an external reference and counter electrode, which makes the setup quite bulky. Additionally, supporting electrolyte was required, complicating sample preparation steps.

In order to detect TNT for real-world applications – e.g. contaminated lakes, rivers or groundwater – it would be highly beneficial to have a miniaturized sensor that can be simply placed in a water sample onsite, without any additional sample preparation steps, or requiring samples to be taken back to the lab for analysis. In this work, a new simple-to-use method to detect TNT in aqueous samples via liquid/liquid partitioning is presented. A strongly hydrophobic gel polymer electrolyte material (ionic liquid and polymer) is used to preconcentrate TNT from the aqueous phase, and transport it to the electrode to be detected. It is shown that by

careful choice of the RTIL and polymer structure, the composite material can be placed directly into aqueous samples, and applied to detect TNT at analytically useful concentrations.

Experimental

Chemicals and Reagents

Trihexyltetradecylphosphonium bis(trifluoromethylsulfonyl)imide ($[P_{14,6,6,6}][NTf_2]$) was used as received after being kindly donated by Professor Christopher Hardacre, formerly at Queen's University Ionic Liquids Laboratory, Belfast, UK and now at the University of Manchester, UK. 1-butyl-3-methylimidazolium bis(trifluoromethylsulfonyl)imide, 99.5 % ($[C_4mim][NTf_2]$) was obtained from IoLiTec (Ionic Liquids Technologies GmbH, Heilbronn, Germany). Poly(methyl methacrylate) (PMMA) was obtained from Sigma-Aldrich as a white powder and contained an average molecular weight of ~15,000, determined by gel permeation chromatography. Poly(hexyl methacrylate) (PHMA) was synthesized from hexyl methacrylate (HMA, 99 %, Sigma-Aldrich Pty Ltd., NSW, Australia) following published procedures,¹⁸ using thermally initiated free radical solution polymerization at 85 °C for 16 h. Full details on the synthesis, and a size exclusion chromatogram for PHMA is provided in the Supporting Information. Ultrapure water with a resistance of 18.2 MΩ cm⁻¹ was obtained from a Millipore Pty. Ltd. laboratory water purification system (North Ryde, NSW, Australia). Acetone (CHROMASOLV®, for HPLC, ≥99.9 %, Sigma-Aldrich) was used for washing electrodes prior to use. A 1000 µg/mL standard of TNT in acetonitrile was obtained from Chem Service, West Chester PA (lot 3196300). A solid TNT sample was kindly donated by the Forensic Science Laboratory at ChemCentre, Perth, Western Australia, through the supervision of Dr David DeTata, and used as received. Ferrocene (Fc, 98 % purity) was obtained from Sigma-Aldrich. A 1 M stock solution of H₂SO₄ (prepared with ultrapure water from a 95–98 wt % H₂SO₄ solution, Ajax Finechem, WA, Australia) was used for activation of the thin-film electrode surfaces. Potassium chloride (KCl, SigmaUltra > 99.0 %) was obtained from Sigma-Aldrich. High-purity nitrogen gas (99.99 %) for sample purging, and high-purity oxygen gas (O₂, 99.5 %) were obtained from BOC Gases (North Ryde, NSW, Australia).

Preparation of Gel-Polymer Electrolytes

Gel-polymer electrolytes (GPEs) were prepared using a similar method reported previously for PMMA- $[C_2mim][NTf_2]$.¹⁹ Four GPEs were examined in this work, using combinations of two RTILs – $[C_4mim][NTf_2]$ and $[P_{14,6,6,6}][NTf_2]$ – and two polymers – PMMA and PHMA. To determine the mass of polymer necessary to gel the RTIL (i.e. so it is mechanically stable), mass ratios of 10, 20, 30, 40, and 50 % m_{pol}/m_{tot} were examined, where m_{pol} is the mass of the polymer (in g) and m_{tot} is the total mass (polymer and RTIL, in g). One of the four mixtures (PHMA/ $[C_4mim][NTf_2]$) did not form a homogeneous, clear gel, so this combination was omitted. Full details of the masses used for the other three mixtures are given in the Supporting Information. 12 µL of the resulting GPE mixtures (using acetone as carrier solvent where necessary) were dropcast onto a glass slide, and left for ~3 hours (h) for any

residual acetone to evaporate. The slide was then held vertically for 12 h to examine the mechanical stability of the mixtures; photos are provided in the Supporting Information (Figures S-1 and S-2). The glass slide is used to simulate the glass substrate of the TFEs used in the electrochemistry experiments.

To test the stabilities of the GPEs in water, the three GPEs at the appropriate mechanically-stable mixing ratios (50 % PMMA- $[C_4\text{mim}][\text{NTf}_2]$, 40 % PMMA- $[P_{14,6,6,6}][\text{NTf}_2]$ and 50 % PHMA- $[P_{14,6,6,6}][\text{NTf}_2]$) were dropcast onto a single glass slide and immersed in ultrapure water, with the slide periodically removed at time periods of 5, 15, 30, 60 min, 2, 4, 6, 8, and 20 h. After each removal, any excess water droplets were blotted away using lint-free tissue paper and the glass slide was photographed. Following the last immersion timeslot, the glass slide was left to dry in air at laboratory room temperature (21 ± 1 °C), photographing after 20 h and 2 weeks (wks).

Water-RTIL extraction experiments

For the extraction of TNT into the RTIL from aqueous samples using the ‘shaking’ method, 1.9 mg of solid TNT was added to 20 mL ultrapure water and was sonicated to dissolve. 200 μL $[C_4\text{mim}][\text{NTf}_2]$ was added, the vial was shaken vigorously for 5 minutes (min) and then left for 20 h to allow for phase separation. The same process was repeated for $[P_{14,6,6,6}][\text{NTf}_2]$, with centrifuging for 10 min at 4000 rpm required for full phase separation with this ionic liquid. 25 μL of the lower RTIL layer was removed and used for analysis on a microdisk electrode (details below). A schematic of this process is shown in Figure 1.

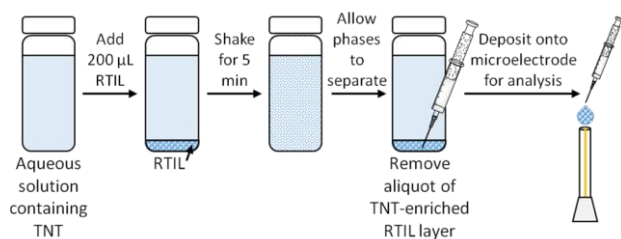


Figure 1. Schematic of the method used to extract TNT from aqueous solution by shaking with an aliquot of room temperature ionic liquid (volumes not to scale) in a glass vial.

Water-GPE extraction experiments

GPE-functionalized TFEs were preconditioned by immersing in water for 15 min, before removal, drying under nitrogen for 1 h and recording a blank square wave voltammogram. To prepare a calibration curve, a cumulative concentration method was employed: 13.5 μL of TNT standard in MeCN (1000 $\mu\text{g}/\text{mL}$) was placed under a gentle stream of nitrogen to evaporate the MeCN before reconstituting with 6.75 mL Milli-Q water, giving a concentration of 2 $\mu\text{g}/\text{mL}$ (aq). Two 0.675 mL aliquots were diluted with an equal volume of water to give two 1.35 mL aliquots of 1 $\mu\text{g}/\text{mL}$ aqueous TNT solutions. A further four 1.35 mL aliquots of 2 $\mu\text{g}/\text{mL}$ TNT were separated into vials. Since TNT can adsorb to glassware, all solutions were sonicated at room temperature for 1 min to ensure full dissolution. A 50 % PHMA- $[P_{14,6,6,6}][\text{NTf}_2]$ -functionalized TFE was immersed in 1 $\mu\text{g}/\text{mL}$ TNT solution using the setup shown in

Figure S-3 in the Supporting Information. The solution was stirred vigorously using a magnetic stirrer for 15 min, after which time the TFE was removed and dried for 15 min under nitrogen, then subjected to SWV analysis. The process was then repeated in a second 1 $\mu\text{g}/\text{mL}$ TNT solution, followed by four 2 $\mu\text{g}/\text{mL}$ solutions to give cumulative exposure to 2, 4, 6, 8 and 10 $\mu\text{g}/\text{mL}$ TNT. This generated a 6-point cumulative calibration curve, with three replicates performed, keeping conditions as similar as possible by maintaining the same positioning of the experimental setup, and using a constant stirring speed.

Electrochemical experiments

All electrochemical experiments were performed using an Autolab PGSTAT101 potentiostat (Eco-Chemie, Netherlands) interfaced to a PC operating Nova 1.11 software. A custom-built aluminium Faraday cage was used to reduce background interference. Gold electrodes were employed rather than platinum, due to the occurrence of electrode fouling for TNT reported on platinum surfaces.^{8,20} For experiments where potential referencing to the ferrocene/ferrocenium (Fc/Fc^+) redox couple was performed, ferrocene was added in-situ from a 25 mM solution in acetonitrile, allowing the acetonitrile to evaporate, leaving a concentration of ferrocene of ca. 3 mM in the RTIL. Potentials were then shifted based on the potential separation from the midpoint of the Fc/Fc^+ redox couple for cyclic voltammetry (CV) and to the Fc^+ reduction peak for square wave voltammetry (SWV). Unless otherwise stated, all CV scans were performed at 100 mVs^{-1} with a step potential of 2 mV. For SWV experiments, optimized parameters were: frequency of 25 Hz, amplitude of 25 mV, and step potential of 4 mV. The temperature of the laboratory was $22 (\pm 1)$ °C.

Microdisk electrode experiments

For water-RTIL (liquid-liquid) extraction experiments, a home-made gold microdisk electrode with a radius of 10.8 μm was employed. The microdisk electrode was used as opposed to the TFE for two reasons: (i) to allow for chronoamperometric analysis using the Shoup and Szabo expression,²¹ and (ii) to use the setup that enables small volumes of RTIL to be placed under vacuum to easily remove dissolved water.^{22,23} The radius was electrochemically calibrated using the steady-state voltammetry of a 3.3 mM solution of $\text{K}_3[\text{Fe}(\text{CN})_6]$ in 0.1 M KCl (aq). Prior to each use, the microelectrode was polished in a figure-8 motion on soft velvet polishing pads (Buehler, Illinois), using sequentially decreasing alumina particle sizes (3 μm , 1 μm and 0.05 μm , Kemet, Marayong, NSW). A section of a disposable plastic micropipette tip was secured at the top of the microelectrode, to create a cavity into which the water-saturated RTIL (typically 20-25 μL) was placed. The electrode was positioned into a glass T-cell,^{22,23} with a silver (Ag) wire (combined reference/counter electrode) inserted in from the top. Prior to each use, the silver wire was cleaned by sonication in acetone for 5 min. The cell was evacuated for ca. 1 h using an Edwards high vacuum pump (model ES 50) to remove dissolved impurities (O_2 , water etc.) from the sample. Cyclic voltammetry was performed to observe the three reduction peaks expected for TNT.⁸ Potential step chronoamperometry was then employed, stepping from 0 V to an appropriate potential after the first reduction peak. To determine the concentration of

TNT in the resulting sample, chronoamperometric transients were fitted to the Shoup and Szabo equation²¹ using the software program Origin 7.5 and diffusion coefficients obtained previously.⁸

Thin-film electrode experiments

TFEs with gold (Au) working, reference and counter electrodes were obtained from Micrux Technologies, Oviedo, Spain (ED-SE1-Au). A custom-made TFE adapter was employed (see Figure S-4 in the Supporting Information) to connect the electrodes in a 3-electrode configuration. All TFEs were electrochemically activated prior to use as recommended by the manufacturer: 12 μL of 1M H_2SO_4 was used to cover the three electrodes, and ~ 100 repeated CV cycles were performed at 1.1 V to -1.2 V at 1000 mVs^{-1} . The TFE was removed from the adapter, washed with ultrapure water and acetone, before drying under a stream of nitrogen.

For TFE experiments in the absence of a polymer, a 2 μL aliquot of RTIL sample of interest was used. For experiments with a GPE, a 3 μL aliquot (after acetone evaporation) was used. This was due to the different viscosity and hydrophobicity of the GPE compared to the neat RTIL, resulting in less spreading over the three electrodes. Once prepared, the TFEs were inserted into one arm of a glass cell^{22,23} and kept under a constant stream of nitrogen gas (0.2 L/min, modulated with a gas flow controller). Prior to analysis, samples of neat RTILs were purged under nitrogen for at least 20 min, while the GPEs were purged for at least 1 h.

3 mM TNT in the GPEs was made using an appropriate volume of the TNT/acetonitrile standard and allowing the acetonitrile to evaporate under nitrogen. Solutions were dropcast onto the TFEs using an equal volume of acetone. To assess the effect of oxygen, 21 % O_2 gas (nitrogen fill) was introduced into the cell using a gas-mixing system described previously.²⁴

Safety Considerations

This work involves the use of explosive materials. Caution must be exercised when dealing with any explosive compounds by removing any initiation sources, using low quantities of material and eliminating any possible friction or impact sources within the experimental vicinity. TNT standards must be stored in a refrigerator or freezer, with solid TNT stored in an explosives safe until removal of a small quantity for experimental purposes.

Results and Discussion

Two RTILs were chosen for this work – $[\text{C}_4\text{mim}][\text{NTf}_2]$ and $[\text{P}_{14,6,6,6}][\text{NTf}_2]$. $[\text{C}_4\text{mim}][\text{NTf}_2]$ has previously been demonstrated to be a promising RTIL for TNT analysis at relatively high concentrations (3-500 mM), allowing for the proposal of an EC_2 reaction mechanism.⁸ $[\text{P}_{14,6,6,6}][\text{NTf}_2]$ was used as a very hydrophobic RTIL, important for the intended application of this work involving direct immersion into aqueous solutions. Figure 2 compares SWVs for 3 mM TNT in the two ionic liquids on a gold TFE. Due to the use of a gold quasi-reference electrode built into the TFE, the potential axis was shifted to the reduction potential of the ferrocenium ion (Fc^+); solutions were analyzed separately in the presence of ferrocene and adjusted so that the Fc^+ reduction peak is at 0 V. Higher peak currents were obtained in

$[\text{C}_4\text{mim}][\text{NTf}_2]$ compared to $[\text{P}_{14,6,6,6}][\text{NTf}_2]$, likely due to the lower viscosity of $[\text{C}_4\text{mim}][\text{NTf}_2]$; diffusion coefficients of TNT in $[\text{P}_{14,6,6,6}][\text{NTf}_2]$ and $[\text{C}_4\text{mim}][\text{NTf}_2]$ are $0.86 \times 10^{-11} \text{ m}^2 \text{ s}^{-1}$ and $2.6 \times 10^{-11} \text{ m}^2 \text{ s}^{-1}$, respectively,⁸ reflecting the different viscosities of the RTILs. Figure 2 also shows that the first reduction peak of TNT (labeled peak I) lies at a more negative potential in $[\text{P}_{14,6,6,6}][\text{NTf}_2]$ (-1.10 V) compared to $[\text{C}_4\text{mim}][\text{NTf}_2]$ (-1.02 V), consistent with the trend reported previously.⁸ This is thought to be due to the stronger interaction of the relatively planar TNT molecule with the planar imidazolium cation, compared to the bulky tetraalkylphosphonium cation, making the reduction slightly easier in the imidazolium RTIL. The potential separations of the three peaks (I, II, and III) in Figure 2 vary significantly in the two RTILs, reflecting their different chemical properties, and highlights the possibility for discriminatory sensing, as will be demonstrated later for TNT samples in the presence of oxygen.

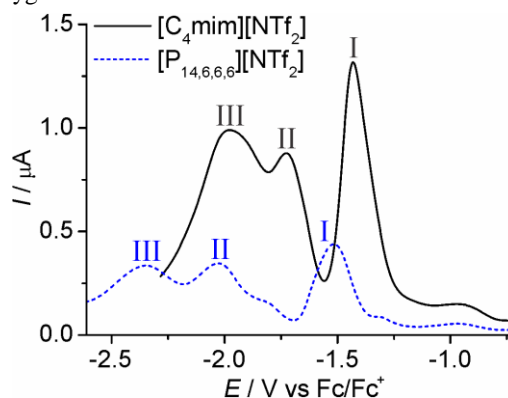
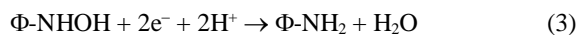


Figure 2. Square wave voltammetry (SWV) on a gold thin-film electrode ($\varnothing=1$ mm) for the reduction of ca. 3 mM TNT in: $[\text{C}_4\text{mim}][\text{NTf}_2]$ (black solid line) and $[\text{P}_{14,6,6,6}][\text{NTf}_2]$ (blue dashed line) in the presence of ferrocene (ferrocenium reduction peak adjusted to 0 V) using a gold reference electrode.

Extraction of TNT from aqueous samples into neat RTILs

To demonstrate the ability of RTILs to extract and preconcentrate TNT from aqueous solutions, a saturated solution of TNT was vigorously shaken with a small volume of RTIL. The resulting RTIL was examined on a gold microdisk electrode. Figure 3 shows cyclic voltammetry (CV) for the reduction of phase-transferred TNT in the two RTILs. Figures 3a and 3c are the CVs in the ‘wet’ RTILs, taken directly from the vial, and Figures 3b and 3d are the same samples dried under vacuum conditions for 1 h (‘dry’). In these experiments, potentials were not referenced to the Fc/Fc^+ redox couple due to the presence of water influencing the ferrocene oxidation peak shape; only peak shapes and currents for TNT are compared. For the ‘wet’ $[\text{C}_4\text{mim}][\text{NTf}_2]$ sample (3a), although there are clearly reductive processes present, there are no distinct reduction peaks as would be expected for TNT in this RTIL.⁸ In the ‘wet’ $[\text{P}_{14,6,6,6}][\text{NTf}_2]$ (3c), there are two reduction peaks present, but a third reduction peak is not obvious even at potentials more negative than -2.2 V. Despite this, the presence of a clear first reduction peak in the ‘wet’ $[\text{P}_{14,6,6,6}][\text{NTf}_2]$ is encouraging and indicates that less drying time may be needed for the more hydrophobic RTIL.

In the ‘wet’ water-saturated RTILs, it is possible that the reaction mechanism may be altered due to the presence of water. Vu et al. suggested that the following reaction scheme takes place for each of the nitro groups when protons (from the solvent) are present:¹⁷



In $[\text{C}_4\text{mim}][\text{NTf}_2]$, this mechanism is indeed possible for the first reduction peak, as indicated by the large (ca. 10 times) increase in current for peak I from the ‘dry’ to the ‘wet’ RTIL. However, in $[\text{P}_{14,6,6,6}][\text{NTf}_2]$, the current of peak I only increases by ca. 1.5 times, suggesting that the full 6-electron reduction does not take place in this more hydrophobic RTIL. This could be due to less water in $[\text{P}_{14,6,6,6}][\text{NTf}_2]$ available to participate in the follow-up chemical reactions. The mechanism in $[\text{P}_{14,6,6,6}][\text{NTf}_2]$ (both ‘wet’ and ‘dry’) could also be complicated by reaction with the phosphonium salt itself, as reported by Compton’s group^{25,26} for the reduction of oxygen to superoxide in an ionic liquid with the same cation. In their work, it was suggested that superoxide is a strong base capable of deprotonating the solvent (phosphonium).^{25,26} For TNT however, it is unlikely that the radical anion deprotonates the solvent (at least on the voltammetric timescale) as indicated by the strong chemical reversibility of the first reduction peak, demonstrated in our previous work.⁸

Upon evacuation of the system for 1 h using a high vacuum pump (to remove dissolved oxygen and water), the resulting voltammetry gave peaks resembling those expected⁸ for TNT (Figure 3b). This suggests that for analysis of TNT in wet RTILs (particularly for $[\text{C}_4\text{mim}][\text{NTf}_2]$), samples should be thoroughly dried to enable clearer visualization of any TNT peaks present. Overall, these results show that $[\text{C}_4\text{mim}][\text{NTf}_2]$ and $[\text{P}_{14,6,6,6}][\text{NTf}_2]$ are both highly suitable solvents for the extraction and preconcentration of TNT from aqueous solutions.

Chronoamperometry was also performed to determine the concentration of TNT within the resulting RTIL layer, along with the percentage recovery of TNT. Diffusion coefficients from Kang et al.⁸ were used, and the chronoamperometric transient was fitted to the Shoup and Szabo equation.²¹ Concentrations of 32 mM in $[\text{C}_4\text{mim}][\text{NTf}_2]$, and 23 mM in $[\text{P}_{14,6,6,6}][\text{NTf}_2]$ were calculated, giving a recovery of ~ 40 % and ~ 29 % in the two RTILs, respectively. These relatively high TNT recoveries demonstrate the strong preference of TNT to partition into the RTIL phase from the aqueous phase, and highlight the promising ability of the RTILs to preconcentrate TNT. It is noted that full recovery is not expected due to the partial solubility of the RTILs in water;²⁷⁻²⁹ we observed RTIL volume loss during the shaking experiments (e.g. only 65 μL was recovered from a starting volume of 200 μL in $[\text{C}_4\text{mim}][\text{NTf}_2]$, see table S-3 of the Supporting Information). Longer settling times resulted in less recovery (e.g. ~ 28 % after 20 h in $[\text{C}_4\text{mim}][\text{NTf}_2]$), and a more intense pink color of the RTIL, indicating possible byproduct formation in the water-saturated RTIL.

Exclusion of Oxygen Interference

If an analyte redox reaction occurs in the reductive potential range, it is highly likely that oxygen will be present as an interferent. Therefore, the electrochemical behavior of oxygen in the two RTILs was examined and compared to that of TNT. Figure 4 shows overlaid CVs for 3 mM TNT (black solid line) and 21 % O_2 (ambient concentration of oxygen in air, blue dashed line), referenced to the midpoint of the ferrocene/ferrocenium redox couple. Oxygen is well-known to reduce to superoxide in a one-electron step in RTILs;^{24,30} superoxide is subsequently oxidized on the reverse scan. In $[\text{C}_4\text{mim}][\text{NTf}_2]$ (Figure 4a), the onset of the oxygen reduction peak occurs before the first reduction peak of TNT. This suggests that the peak current for TNT will be increased in the presence of oxygen, leading to the possibility of incorrect readings. In contrast, in $[\text{P}_{14,6,6,6}][\text{NTf}_2]$ (Figure 4b), the oxygen reduction peak is at a much more negative potential than the TNT reduction peak, and there appears to be no observable current from oxygen at the potential of TNT reduction peak I. The reason for this is likely to be due to the very different solvation of oxygen and superoxide molecules with different RTIL cations (cf. Marcus theory),³¹ giving rise to vastly different kinetics of the electrochemical step.

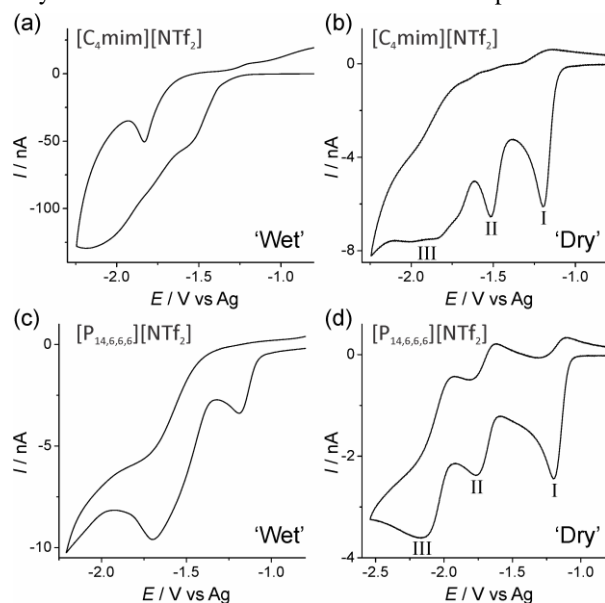


Figure 3. CVs on a gold microelectrode (diameter 21.6 μm) at a scan rate of 100 mVs^{-1} following 5 min shaking with an aqueous solution of saturated TNT: (a) ‘wet’ $[\text{C}_4\text{mim}][\text{NTf}_2]$, (b) ‘dry’ $[\text{C}_4\text{mim}][\text{NTf}_2]$, (c) ‘wet’ $[\text{P}_{14,6,6,6}][\text{NTf}_2]$, and (d) ‘dry’ $[\text{P}_{14,6,6,6}][\text{NTf}_2]$. ‘Wet’ refers to freshly extracted water-saturated RTILs, and ‘dry’ refers to the same solutions placed under vacuum for 1 hour.

Table 1 shows the peak-to-peak separations (ΔE_p) of the oxygen/superoxide redox couple and TNT reduction peak I (data for TNT was obtained when CV was reversed after peak I). For TNT, the RTIL cation has a smaller influence on the kinetics than for oxygen, where the oxygen/superoxide redox couple has a very wide ΔE_p of 588 mV in $[\text{P}_{14,6,6,6}][\text{NTf}_2]$, 317 mV wider than for $[\text{C}_4\text{mim}][\text{NTf}_2]$. Large ΔE_p values for the oxygen/superoxide redox couple are common in ionic liquids, and are known to vary significantly

between different RTILs.^{24,25} Additionally, as shown in Table 1, there is a 420 mV separation between the TNT and oxygen peaks in [P_{14,6,6,6}][NTf₂], but only 170 mV in [C₄mim][NTf₂].

Table 1. Reduction potentials (E_{red}) and peak-to-peak separations (ΔE_p) for 21 % O₂ and 3 mM TNT (peak I) in the two RTILs using CV at 100 mVs⁻¹ on a gold TFE.

RTIL	Oxygen reduction		TNT reduction (peak I)	
	E_{red} / V (vs Fc/Fc ⁺)	ΔE_p / V	E_{red} / V (vs Fc/Fc ⁺)	ΔE_p / V
[C ₄ mim][NTf ₂]	-1.23	0.271	-1.06	0.093
[P _{14,6,6,6}][NTf ₂]	-1.63	0.588	-1.21	0.124

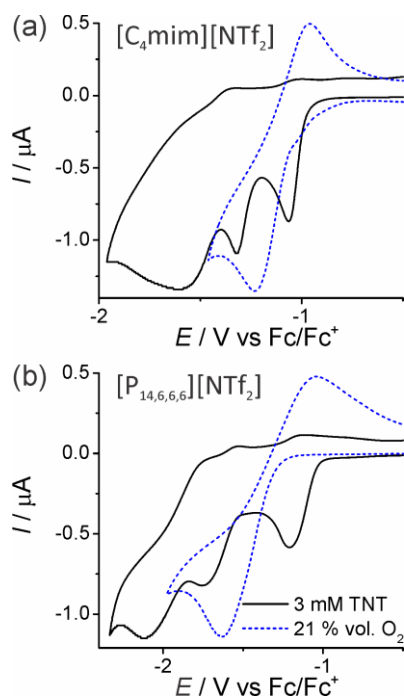


Figure 4. CVs on a gold thin-film electrode ($\varnothing=1$ mm) at a scan rate of 100 mVs⁻¹ for: a) 3 mM TNT in [C₄mim][NTf₂] under N₂ (solid line), and 21% O₂ in [C₄mim][NTf₂] (dashed line); b) 3 mM TNT in [P_{14,6,6,6}][NTf₂] under N₂ (solid line) and 21% O₂ in [P_{14,6,6,6}][NTf₂] (dashed line).

To test the influence of oxygen on the measured current of TNT peak I, 3 mM TNT was examined in the presence of 21 % O₂. The peak current was measured at E_{red} for TNT peak I (given in Table 1). In [C₄mim][NTf₂], an increase in peak current was observed when 21 % O₂ was present; the current was 45 % higher than in nitrogen. However, in [P_{14,6,6,6}][NTf₂], the TNT peak I current did not change significantly in the presence of oxygen, giving rise to only a 2 % increase in current with 21 % O₂ (see Figure S-5 in the Supporting Information). This suggests that for TNT sensing, [P_{14,6,6,6}][NTf₂] is far superior to [C₄mim][NTf₂] in a typical air environment. It is not unusual to observe differing voltammetric responses in different RTILs and these results therefore suggest that a superior electrolyte may be identified

for the detection of TNT (or other analytes) by careful tuning of the ionic liquid structure.

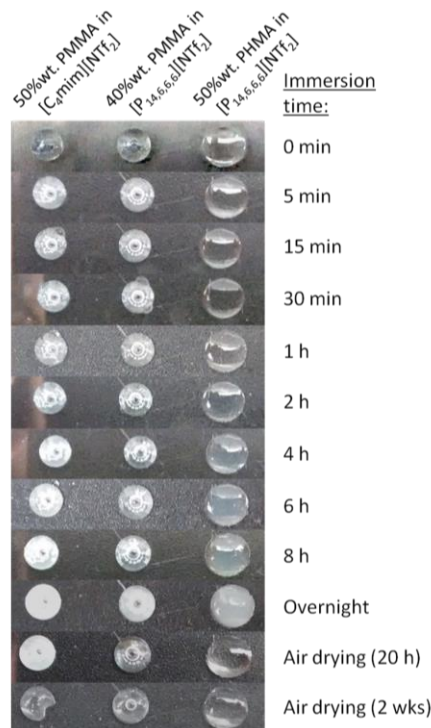


Figure 5. Photographs of the three GPEs after increasing immersion times in ultrapure water, followed by removal and drying at room temperature for 20 hours and two weeks.

Optimizing GPE mixing ratios, and their water immersion behavior

After determining that both [C₄mim][NTf₂] and [P_{14,6,6,6}][NTf₂] are suitable for the extraction of TNT from aqueous solutions, and assessing the response of TNT in the presence of oxygen, the next stage towards making a robust, portable sensor is to make the electrolyte ‘spill-less’ by mixing with a polymer. Two polymers were assessed: poly(methyl methacrylate) (PMMA) and poly(hexyl methacrylate) (PHMA). PMMA is an electrochemically inert polymer that has previously been shown to form gel polymers with [C₂mim][NTf₂], where it was used with a Pt TFE for oxygen sensing.²⁴ In addition, a structurally similar polymer – PHMA – was used, which is more hydrophobic than PMMA, and should be more suitable for direct immersion into aqueous samples, as discussed later. Four polymer/RTIL combinations were prepared, but only three of these (PMMA/[C₄mim][NTf₂], PMMA/[P_{14,6,6,6}][NTf₂] and PHMA/[P_{14,6,6,6}][NTf₂]) formed transparent, homogeneous gel-like polymers as desired. The three combinations at various concentrations (10-50 % polymer by mass) were drop-cast onto a glass microscope slide and held in a vertical orientation for 12 h to assess the adhesion properties to glass over extended periods of time (see Figures S-1 and S-2). Mixing ratios of 50 %, 40 %, and 50 % (by mass), respectively, were chosen as appropriate ratios where the GPEs remained mechanically stable in a vertical orientation (i.e. did not flow).

The three optimized GPE combinations were dropcast onto a single glass slide and their water immersion behavior was assessed. Figure 5 shows photographs of the three GPEs at increasing immersion times. All GPEs began to turn white and opaque at increasing immersion times. A possible reason for the white color could be due to RTIL leaching into the bulk water phase, with the white color resembling that of the pure polymers. However, upon closer inspection, their surfaces had a sheen reminiscent of an emulsion. Therefore, it is hypothesized that water molecules may have partitioned into the outermost layer of the gel droplet. The onset of opacity was fastest for the least hydrophobic PMMA and [C₄mim][NTf₂] GPEs, and slowest for the most hydrophobic GPE, PHMA/[P_{14,6,6,6}][NTf₂]. After being left to dry in air for 20 h and 2 wks, respectively (bottom two rows of Figure 5), it can be seen that the most hydrophobic GPE almost reverted back to its original transparent appearance. On the other hand, the PMMA-based GPEs required much longer. It is likely that the water penetration layer was more closely confined to the surface for the more hydrophobic gel polymer combination, resulting in a shorter drying time, consistent with the CV results presented in Figure 3.

Analytical Utility: GPE-TFEs for TNT detection in aqueous samples

The optimum combination of hydrophobic polymer and hydrophobic ionic liquid – PHMA/[P_{14,6,6,6}][NTf₂] – was used as a GPE for direct immersion into aqueous solutions of TNT. The GPE was dropcast on a gold TFE to cover all three electrodes, and the electrolyte was then preconditioned by immersing in water for 15 min, dried for 1 h under a stream of nitrogen, before recording a blank SWV. Without the preconditioning step, blank voltammograms had very different background currents to the TNT partitioned samples.

A single TFE was then immersed in several 1 µg/mL and 2 µg/mL aqueous solutions of TNT and stirred for 15 min at each concentration and dried for 15 min in nitrogen (see experimental section for full details). This method relies on the assumption that the TNT partitions into and remains in the gel polymer over time due to its high solubility in the ionic liquid. Before the drying step, currents were around 10 % higher, but stabilized to a constant value after 15 minutes. The total time taken to record one measurement was therefore around 30 minutes, making field based detection possible with this method. Figure 6a shows SWV for cumulative concentrations of 1–10 µg/mL (TNT peak I only), fit to a linear baseline at -0.3 to -0.4 V. At the lowest concentration studied (1 µg/mL), CVs of the same systems showed highly resistive (sloping) behavior and the TNT peaks were not obvious. On the other hand, SWV showed clear TNT peaks and a high stability upon repeated SWV analysis at 15 min intervals. A cumulative TNT calibration graph was recorded, measuring the current of peak I, fitting a 2nd order polynomial spline around the peak to account for the noise. The increased noise is likely due to the low currents measured (close to the limits of the standard potentiostat) and the use of a highly viscous gel polymer electrolyte. A further two replicates were performed on separate GPE/gold TFE sample preparations, and the averaged data of peak current vs. cumulative concentration is shown in Figure 6b, with error bars corresponding to one standard deviation. The equation of the

best fit line was $I(\text{nA}) = 2.84 \times 10^{-11} \times [\text{TNT}] (\mu\text{g/mL}) - 9.85 \times 10^{-12}$ and the limit of detection (based on three times the standard deviation of the line) was calculated to be 0.37 µg/mL. This is significantly lower than the typical concentrations of TNT found in contaminated groundwater.^{1,32,33}

To further validate the method, three samples at the highest concentration (10 µg/mL) were separately analysed without the cumulative steps. Current responses were similar to those recorded using the cumulative method (see red cross with error bars on Figure 6b), suggesting that quantitative detection is indeed possible with this sensor.

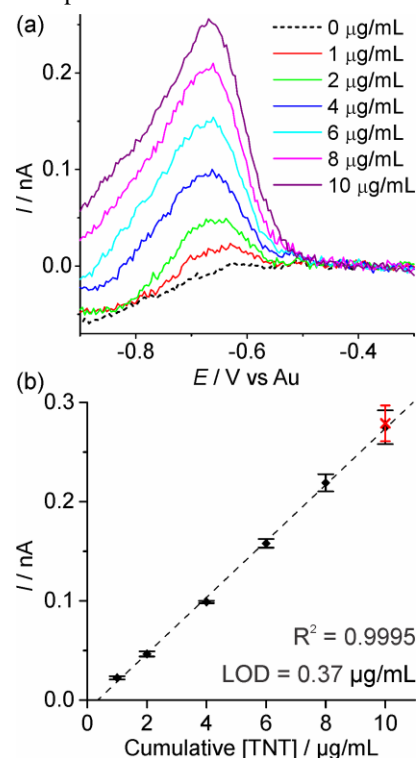


Figure 6. (a) SWVs on a gold TFE (WE Ø=1 mm) for the first reduction peak of TNT. TNT was partitioned into the GPE from aqueous phase concentrations of 1–10 µg/mL, each with a 15 minute GPE immersion/stirring time. (b) Corresponding cumulative calibration plot averaged from three separate TFEs, with error bars of one standard deviation. The red data point shows the response of three repeat 10 µg/mL samples without the accumulation steps.

To confirm that the TNT did not leach out from the GPE after its partitioning, the sensor was immersed in pure water, stirred vigorously for 15 min and subsequently analyzed using SWV. The peak current was comparable before and after immersion, suggesting that TNT has a strong preference for the gel polymer and will remain there following its initial partitioning. This suggests that these sensors can be considered as disposable devices, and can be discarded once they have been used to quantify a TNT sample. The low cost of the TFEs and minimal amounts of material required means that these sensors should be highly suitable for this purpose.

Finally, a bare gold TFE (with no GPE) was used to try to detect TNT directly in aqueous solution (with 0.1 M KCl as a supporting electrolyte). It was found that no TNT could be detected in the absence of the gel polymer, confirming that

the presence of the gel polymer is necessary to preconcentrate the TNT in solution prior to its detection. Additionally, the use of the GPE modified device means that no sample preparation is required once the GPE is deposited onto the electrode device. This reduces the complexity of the system and avoids the need to make up any additional solutions prior to analysis, which could be difficult for onsite samples.

Conclusions

The detection and quantification of TNT in aqueous solutions has been demonstrated using a miniaturized planar electrode with a hydrophobic gel polymer electrolyte. Initially, SWV of TNT dissolved directly in two RTILs revealed different behavior when the RTIL cation is changed, suggesting the possibility of discriminatory sensing by tuning of the RTIL structure. Shaking experiments were performed to demonstrate the partitioning of TNT across the water/RTIL interface, and the preconcentration ability of the RTIL. Using CV, phase-transferred TNT was observed in the RTIL, with different responses in the wet and dry samples, suggesting that drying is necessary, particularly in the less hydrophobic RTIL [C₄mim][NTf₂]. The voltammetry of TNT was also much less affected by oxygen in the RTIL [P_{14,6,6,6}][NTf₂] compared to [C₄mim][NTf₂], suggesting that [P_{14,6,6,6}][NTf₂] is the superior electrolyte of the two RTILs.

To construct a robust sensor, gel polymer electrolytes were made using two simple polymers, PMMA and PHMA, and the [P_{14,6,6,6}][NTf₂]/PHMA combination showed the best stability when immersed in water for extended periods of time. This combination was thus used as an electrolyte to generate a cumulative calibration graph at TNT concentrations of 1–10 µg/mL. Linear behavior was observed, with a limit of detection of 0.37 µg/mL, well below the typical values found in TNT-contaminated groundwater. The sensor device is low-cost, robust, disposable, and highly portable and the sampling method is convenient and rapid. This approach could transform TNT detection at scenes without any additional sample preparation steps prior to analysis. Future work will involve applying this sensor for the detection of TNT in real samples (e.g. contaminated soils and water) in collaboration with appropriate environmental agencies.

Supporting Information

Experimental details for the synthesis of PHMA. Density of the RTILs and polymers used, and mass/volumes employed to make up the GPEs. Photographs of 10–50 % (polymer by mass) of GPEs on a glass slide in flat and vertical orientations. Photograph of the custom-made electrode adaptor, and instrumental configuration used for the calibration experiments. Word document. This material is available free of charge via the Internet at <http://pubs.acs.org>.

AUTHOR INFORMATION

Corresponding Author

*E-mail: d.silvester-dean@curtin.edu.au. Tel.: +61 (0) 892667148. Fax: +61 (0) 892662300.

Author Contributions

All authors have given approval to the final version of the manuscript.

ACKNOWLEDGMENT

The authors thank Prof. Christopher Hardacre for the kind donation of the tetraalkylphosphonium ionic liquid, and Dr. David DeTata for the donation of the solid TNT sample used in this work. H.A.Y. thanks Curtin University for a Curtin International Postgraduate Research Scholarship (CIPRS). D.S.S. thanks the Australian Research Council for a Discovery Early Career Researcher Award (DECRA: DE120101456).

REFERENCES

- (1) Pichtel, J. *Appl. Environ. Soil Sci.* **2012**, *2012*, 1–33.
- (2) Lefferts, M. J.; Castell, M. R. *Anal. Methods* **2015**, *7*, 9005–9017.
- (3) Cetó, X.; O'Mahony, A. M.; Wang, J.; del Valle, M. *Talanta* **2013**, *107*, 270–276.
- (4) Wang, J. *Electroanalysis* **2007**, *19*, 415–423.
- (5) Silvester, D. S. *Analyst* **2011**, *136*, 4871–4882.
- (6) Silvester, D. S.; Aldous, L. In *Electrochemical Strategies in Detection Science*, Arrigan, D. W. M., Ed.; RSC: Cambridge, UK, 2016.
- (7) Rehman, A.; Zeng, X. *RSC Adv.* **2015**, *5*, 58371–58392.
- (8) Kang, C.; Lee, J.; Silvester, D. S. *J. Phys. Chem. C* **2016**, *120*, 10997–11005.
- (9) Chua, C. K.; Pumera, M.; Rulišek, L. *J. Phys. Chem. C* **2012**, *116*, 4243–4251.
- (10) Forzani, E. S.; Lu, D. L.; Leright, M. J.; Aguilar, A. D.; Tsow, F.; Iglesias, R. A.; Zhang, Q.; Lu, J.; Li, J. H.; Tao, N. J. *J Am Chem Soc* **2009**, *131*, 1390–1391.
- (11) Aguilar, A. D.; Forzani, E. S.; Leright, M.; Tsow, F.; Cagan, A.; Iglesias, R. A.; Nagahara, L. A.; Amlani, I.; Tsui, R.; Tao, N. J. *Nano Lett* **2010**, *10*, 380–384.
- (12) Xiao, C.; Rehman, A.; Zeng, X. *Anal. Chem.* **2012**, *84*, 1416–1424.
- (13) Bandodkar, A. J.; O'Mahony, A. M.; Ramirez, J.; Samek, I. A.; Anderson, S. M.; Windmiller, J. R.; Wang, J. *Analyst* **2013**, *138*, 5288–5295.
- (14) Fernández, E.; Vidal, L.; Iniesta, J.; Metters, J. P.; Banks, C. E.; Canals, A. *Anal. Bioanal. Chem.* **2014**, *406*, 2197–2204.
- (15) Guo, C. X.; Lu, Z. S.; Lei, Y.; Li, C. M. *Electrochem Commun* **2010**, *12*, 1237–1240.
- (16) Guo, S. J.; Wen, D.; Zhai, Y. M.; Dong, S. J.; Wang, E. K. *Biosens Bioelectron* **2011**, *26*, 3475–3481.
- (17) Vu, H. T. T.; Le, H. T. V.; Pham, Y. T. H.; Le, H. Q.; Pham, P. H. *Bull. Korean Chem. Soc.* **2016**, *37*, 378–385.
- (18) Qin, Y.; Peper, S.; Bakker, E. *Electroanalysis* **2002**, *14*, 1375–1381.
- (19) Lee, J.; Du Plessis, G.; Arrigan, D. W. M.; Silvester, D. S. *Anal. Methods* **2015**, *7*, 7327–7335.
- (20) Hilmi, A.; Luong, J. H. T.; Nguyen, A.-L. *Anal. Chem.* **1999**, *71*, 873–878.
- (21) Shoup, D.; Szabo, A. J. *J. Electroanal. Chem. Interfacial Electrochem.* **1982**, *140*, 237–245.
- (22) Silvester, D. S.; Wain, A. J.; Aldous, L.; Hardacre, C.; Compton, R. G. *J. Electroanal. Chem.* **2006**, *596*, 131–140.
- (23) Schroder, U.; Wadhawan, J. D.; Compton, R. G.; Marken, F.; Suarez, P. A. Z.; Consorti, C. S.; de Souza, R. F.; Dupont, J. *New J. Chem.* **2000**, *24*, 1009–1015.
- (24) Lee, J.; Murugappan, K.; Arrigan, D. W. M.; Silvester, D. S. *Electrochim. Acta* **2013**, *101*, 158–168.

- (25) Li, P.; Barnes, E. O.; Hardacre, C.; Compton, R. G. *J. Phys Chem. C* **2015**, *119*, 2716-2726.
- (26) Li, P.; Compton, R. G. *Electroanalysis* **2015**, *27*, 1550-1555.
- (27) Freire, M. G.; Neves, C. M. S. S.; Carvalho, P. J.; Gardas, R. L.; Fernandes, A. M.; Marrucho, I. M.; Santos, L. M. N. B. F.; Coutinho, J. A. P. *J. Phys Chem. B* **2007**, *111*, 13082-13089.
- (28) Kurnia, K. A.; Quental, M. V.; Santos, L. M. N. B. F.; Freire, M. G.; Coutinho, J. A. P. *Phys. Chem. Chem. Phys.* **2015**, *17*, 4569--4577.
- (29) Zhou, T.; Chen, L.; Ye, Y.; Chen, L.; Qi, Z.; Freund, H.; Sundmacher, K. *Ind. Eng. Chem. Res.* **2012**, *51*, 6256-6264.
- (30) Zhang, D.; Okajima, T.; Matsumoto, F.; Ohsaka, T. *J. Electrochem. Soc.* **2004**, *151*, D31-D37.
- (31) Compton, R. G.; Banks, C. E. *Understanding Voltammetry*; 1st. Ed., World Scientific: Singapore, 2007.
- (32) Martel, R.; Robertson, T. J.; Doan, M. Q.; Thiboutot, S.; Ampleman, G.; Provatas, A.; Jenkins, T. *Environ. Geol.* **2008**, *53*, 1249-1259.
- (33) Best, E. P. H.; Zappi, M. E.; Fredrickson, H. L.; Sprecher, S. L.; Larson, S. L.; Ochman, M. *Ann. N. Y. Acad. Sci.* **1997**, *829*, 179-194.